RESEARCH PAPER

Synthesis, properties, and application in peptide chemistry of a magnetically separable and reusable biocatalyst

Cleber W. Liria · Vitor A. Ungaro · Raphaella M. Fernandes ·
Natália J. S. Costa · Sandro R. Marana · Liane M. Rossi ·
M. Teresa Machini

Abstract Enzyme-catalyzed chemical processes are selective, very productive, and generate little waste. Nevertheless, they may be optimized using enzymes bound to solid supports, which are particularly important for protease-mediated reactions since proteases undergo fast autolysis in solution. Magnetic nanoparticles are suitable supports for this purpose owing to their high specific surface area and to be easily separated from reaction media. Here we describe the immobilization of bovine α-chymotrypsin (αCT) on silica-coated superparamagnetic nanoparticles (Fe$_3$O$_4$@silica) and the characterization of the enzyme-nanoparticle hybrid (Fe$_3$O$_4$@silica-αCT) in terms of protein content, properties, recovery from reaction media, application, and reuse in enzyme-catalyzed peptide synthesis. The results revealed that (i) full acid hydrolysis of the immobilized protease followed by amino acid analysis of the hydrolyzate is a reliable method to determine immobilization yield; (ii) despite showing lower amidase activity and a lower K_{cat}/K_m value for a specific substrate than free αCT, the immobilized enzyme is chemically and thermally more stable, magnetically recoverable from reaction media, and can be consecutively reused for ten cycles to catalyze the amide bond hydrolysis and ester hydrolysis of the protected dipeptide Z-Ala-Phe-OMe. Altogether, these properties indicate the potential of Fe$_3$O$_4$@silica-αCT to act as an efficient, suitably stable, and reusable catalyst in amino acid, peptide, and protein chemistry as well as in proteomic studies.

Cleber W. Liria, Vitor A. Ungaro, and Raphaella M. Fernandes have contributed equally to this study.

C. W. Liria · V. A. Ungaro · R. M. Fernandes ·
S. R. Marana · M. T. Machini (✉)
Department of Biochemistry, Institute of Chemistry, University of São Paulo, Av. Prof. Lineu Prestes, 748, PO Box 26077, São Paulo, SP 05513-970, Brazil
e-mail: mtmachini@iq.usp.br

N. J. S. Costa · L. M. Rossi
Department of Fundamental Chemistry, Institute of Chemistry, University of São Paulo,
PO Box 26077, São Paulo, SP 05513-970, Brazil

Introduction

The ability of enzymes to catalyze chemical reactions of biological importance or industrial interest with unmatched efficiency and selectivity is well known.

Consequently, these biocatalysts have been extensively used in science and industry (Thomas et al. 2002). Being highly selective, productive, and environmentally friendly, biocatalysis is in harmony with the principles of Green Chemistry and, therefore, has been recognized as clean technology (Aldridge 2013).

Enzymes are generally used for variable purposes in their free form (dissolved in the reaction media) or immobilized on solid supports (insoluble in the reaction media). The practical application of free enzymes is hindered by both high costs and difficulties in enzyme separation and recycling, but immobilization allows enzyme recovery and reuse in batch and continuous flow systems (Chen and Su 2001; Homaei et al. 2013). These technological advances are indispensable for the industrial and analytical application of enzyme-catalyzed reactions (Yamaguchi et al. 2010; Forsberg et al. 2011). Moreover, the immobilization of such biomolecules may improve their thermal and chemical stabilities (Kim et al. 2005; Hong et al. 2006; Hegedus and Nagy 2009; Zhang et al. 2013; Singh et al. 2013) and affect their catalytic properties, such as substrate recognition and binding (Singh et al. 2013).

Enzyme immobilization can be achieved by simple adsorption, ionic affinity, covalent attachment to a solid support, entrapment into a solid matrix or membrane-restricted compartment, and cross-linking involving enzyme molecules (Homaei et al. 2013; Zhang et al. 2013; Faber 1997; Datta et al. 2013). Various supports have been used for this purpose, such as polymers (Li et al. 2013), silica (Bernal et al. 2014), and carbon (Lugo-Morales et al. 2013), which can be separated by filtration and centrifugation. The immobilization of enzymes on nanostructures can be advantageous because it can increase the stability of those proteins, which in the free form have short lifetimes in solution (Kim et al. 2005; Hegedus and Nagy 2009; Flores-Fernández and Griebenow 2012). This is particularly important for proteases, which can undergo autolysis.

Owing to their large specific surface area (area/volume), magnetic nanoparticles are even more suitable for enzyme immobilization (Rossi et al. 2004; Sun et al. 2013). Superparamagnetic nanoparticles (SPM NPs) have attracted attention as supports to be used for such a purpose because they can be manipulated by an applied magnetic field but do not aggregate in its absence (Pankhurst et al. 2003; Netto et al. 2013). Magnetic separation is a robust, highly-efficient, and rapid method of enzyme recovery that greatly simplifies its handling and allows for its recycling.

Some authors of this study have examined protease-catalyzed synthesis of dipeptides (Liria et al. 2008) of high scientific and commercial importance (Christian and Brent 2001) since this method is amino acid racemization-free, cheaper than classical or solid-phase chemical synthesis, and environmentally friendly (therefore more suitable for industrial production). Alanil-phenylalanine, Ala-Phe, was chosen as one of our targets because it has bitter taste and, therefore, potential application in the food industry as substituent of caffeine. Its synthetic route, which has been optimized and will be described elsewhere, comprises the following steps: (1) synthesis of Z-Ala-Phe-OMe using Z-Ala-OH, Phe-OMe.HCl, and free thermolysin; (2) hydrolysis of the ester of Z-Ala-Phe-OMe using αCT to form Z-Ala-Phe-OH; and (3) catalytic hydrogenation of Z-Ala-Phe-OH and formation of desired peptide (Ala-Phe) using palladium heterogeneous catalysis (to be published in detail elsewhere). The cost of this and other dipeptide green syntheses may be significantly reduced by enhancing the stability of the purified biocatalysts used, making easy their separation from reaction media and reuse. Thus, in the present study, bovine α-Chymotrypsin (αCT) was immobilized on silica-coated magnetite (Fe$_3$O$_4$@silica), and the resulting Fe$_3$O$_4$@silica-αCT was characterized in its protein content, amidase activity, chemical and thermal stabilities, possibility of recovery from the reaction media, reuse potential, and ability to catalyze step 2 of the synthetic route cited above.

Experimental

General remarks

The bovine αCT used was purchased from Biobrás Diagnósticos (Brazil). αCT-specific substrates, Nα-benzoyl-D$_L$-tyrosine 4-nitroanilide (Bz-DL-Tyr-pNA), and N-succinyl-alanine-alanine-proline-phenylalanine 4-nitroanilide (Suc-AAPF-pNA) were purchased from Bachem (USA) and Sigma Chemical Company (USA), respectively. The acetonitrile (ACN; Vetec Fine Chemicals Ltd., Brazil) and trifluoroacetic acid (TFA, Merck KGaA, Germany), used

for the preparation of RP-HPLC solvents A and B, were of spectroscopic grade. Tris (hydroxymethyl)-aminomethane (Tris–HCl), calcium acetate, and tri-ethylamine (TEA) were of analytical grade and purchased from Merck KGaA (Germany). Finally, esters of N-α-acyl amino acids (acyl donors) and amino acids (acyl acceptors) were obtained from Bachem (USA).

Synthesis of Z-Ala-Phe-OMe catalyzed by free thermolysin

Thermolysin-catalyzed Z-Ala-Phe-OMe synthesis was based on our previous studies (Miranda and Tominaga 1991; Machini 1985; Miranda et al. 1986) and will be described in detail elsewhere.

Synthesis and functionalization of magnetic support

The synthesis of the magnetic support was performed according to the methodology described by Rossi and coworkers (Jacinto et al. 2008). A volume of 10.0 mL of an aqueous solution of $FeCl_3$ 1.0 mol L^{-1} was added to 2.5 mL of an aqueous solution of $FeCl_2$ 2.0 mol L^{-1} in HCl 2.0 mol L^{-1}, and the resulting mixture was immediately added to 250 mL of a solution of NH_4OH 0.7 mol L^{-1} under an N_2 atmosphere. The mixture was allowed to react while stirred in an Ultra Turrax (Ika, model T18, Staufen, Germany) for 30 min under an N_2 atmosphere. The particles of Fe_3O_4 formed were magnetically recovered and washed with water five times.

The hydrophobicity of Fe_3O_4 nanoparticles was enhanced by coating the particles' surface with oleic acid. For this purpose, a solution of 2.2 g of oleic acid in 5.0 mL of acetone was added to the suspension of particles in water (oleic acid: Fe_3O_4 1.4:1), and the reaction was allowed to occur for 30 min at room temperature under stirring. The particles were then precipitated with acetone, magnetically separated, and washed with acetone three times. They were dispersed in cyclohexane (50 mL) and centrifuged at 2,000 rpm for 30 min. The concentration of oleic acid-coated Fe_3O_4 nanoparticles in the final suspension was ca. 25 g L^{-1}, as determined by gravimetry.

Finally, the magnetic nanoparticles were coated with silica using a reverse microemulsion. Briefly, the mixture containing 89.2 g of poly(oxyethylene)

nonylphenyl ether (IGEPAL CO-520) and 1.4 L of cyclohexane was homogenized by sonication for 5 min. Next, 400 mg of Fe_3O_4 nanoparticles coated with oleic acid (32 mL of nanoparticle suspension in cyclohexane), 19.0 mL of ammonium hydroxide, and 15.4 mL of tetraethoxysilane (TEOS) were added; the reaction occurred for 16 h at room temperature. Then, to promote the separation of silica-coated magnetite NPs from reaction media, 300 mL of methanol was added. The suspension phase containing the magnetic support was separated and centrifuged at 7,000 rpm for 20 min and washed with methanol (1 × 150 mL) and ethanol (2 × 150 mL). The solid was dried in an oven at 100 °C for 24 h to obtain a dry powder (2.5 g). The sample was named Fe_3O_4@silica.

The functionalization of the silica surface was accomplished by the dispersion of 200 mg of the magnetic support in 30.0 mL of toluene, followed by the addition of 300 µL of 3-aminopropyl-triethoxysilane (APTES). After 2 h of stirring, the particles were washed with toluene (3 × 75 mL) and magnetically separated. The obtained solid was dried under vacuum and subsequently in an oven for 20 h at 100 °C. The sample was named Fe_3O_4@silica-NH$_2$.

The quantification of amine groups at the nanoparticles' surface was accomplished by reaction with ninhydrin. For such purpose a calibration curve was first obtained by incubating 1 mL of ninhydrin solution, 5 mL of phosphate buffer (0.1 mol L^{-1}, pH 6.5), and 10 µL of APTES for 1 h in a boiling water bath. After diluting the reaction medium, the absorbance of the resulting solutions was recorded in a spectrophotometer (UV-1601PC, Shimadzu, Kyoto, Japan) at 570 nm. The method was applied to amino- and glutaraldehyde-functionalized nanoparticles. The amount of 50 mg of each sample was suspended in 5 mL of buffer and 1 mL of ninhydrin. After 1 h in a boiling water bath, the solid was magnetically separated and washed with boiling water until the purple color of the supernatant disappeared. The initial supernatant and the washing solutions were transferred to a 100 mL volumetric flask; the volume was then adjusted with water and absorbance at 570 nm was obtained.

Immobilization of αCT

The amino-functionalized magnetic support Fe_3O_4@silica-NH$_2$ (50 mg) was suspended in phosphate

buffer (40 mL, 50 mmol L^{-1}), pH 7.4, containing 10 wt % glutaraldehyde. The resultant suspension was magnetically stirred for 1 h. Then, the solid was separated using magnetic decantation, washed, and resuspended in a phosphate buffer solution containing αCT (0.5 mg L^{-1}). This suspension was stirred (37 °C; 300 rpm) for 2, 4, 8, or 16 h. The αCT immobilized on the magnetic support (named Fe$_3$O$_4$@silica-αCT) was separated by magnetic decantation, washed with water, resuspended in phosphate buffer, and divided into two parts. One part was stored at room temperature (wet Fe$_3$O$_4$@silica-αCT), and the other part was lyophilized and stored at 4 °C (dry Fe$_3$O$_4$@silica-αCT).

Determination of protein content of Fe$_3$O$_4$@silica-αCT by the Bradford method

An aliquot of the supernatant of the immobilization reaction at 0 or 2 h was separated and diluted ten times. A volume of 160 μL of each diluted sample was transferred to the wells of an Enzyme-Linked Immunosorbent Assay (ELISA) 96-well microplate. To each well was added 40 μL of the solution Coomassie® Brilliant Blue G-250, and after 5 min, the absorbance at 595 nm was measured (SpectraMax® Paradigm® Multi-Mode Detection Platform, Wals, Austria). This procedure was repeated 3 times. Protein quantification was achieved using a calibration curve established with bovine serum albumin (Sigma, St. Louis, USA).

Determination of protein content of Fe$_3$O$_4$@silica-αCT by its full acidic hydrolysis followed by amino acid analysis of the hydrolyzate

Samples of Fe$_3$O$_4$@silica-NH$_2$ (negative control), free αCT, and Fe$_3$O$_4$@silica-αCT were submitted to total acid hydrolysis at 130 °C in a Pico-Tag workstation (Waters, USA) in the presence of a 50 % HCl/propionic acid (V/V) and N$_2$ atmosphere for 24 h. The hydrolyzates were dried (for acid removal), dissolved in water, and filtered. The filtrates were analyzed on a Dionex amino acid analyzer (Sunnyvale, USA) composed of an automatic sampler (AS40), a quaternary pump (GS50), a column oven (LC25), an ion exchange column (2 × 250 mm, AminoPac PA10), an electrochemical detector (ED50), and a "Chromeleon" platform for control and data acquisition. The amount of each amino acid was calculated from the analysis of a standard mixture containing 19 amino acids in known concentrations. For the quantification of immobilized and free αCT, the amino acids, Gln, Glu, Asp, and Asn were used as references.

Enzyme activity assay using Bz-DL-Tyr-pNA as substrate

The αCT activity was determined using 4-nitroanilide N-benzoyl α-DL-tyrosine (Bz-DL-Tyr-pNA) as substrate, following Bundy's method (Bundy 1863).

For the free αCT, 0.2 mL of fresh enzyme solution (5.0 g L^{-1} in phosphate buffer pH 7.4) and 2.8 mL of substrate solution (0.4 g L^{-1} in DMSO, acetaldehyde and phosphate buffer 0.07 mol L^{-1} pH 7.4) were incubated under shaking at room temperature. The reaction was monitored in a Shimadzu spectrophotometer (model UV-160 1PC, Kyoto, Japan) coupled to a computer to record the absorbance variation at 405 nm (ΔA_{405}/min).

For wet Fe$_3$O$_4$@silica-αCT, 0.2 mL of Fe$_3$O$_4$@silica-αCT suspension stored at room temperature or at 4 °C (5.0 g L^{-1}) and 2.8 mL of substrate solution (0.4 g L^{-1}) were incubated under shaking at room temperature. After 3 min, the solid was magnetically separated, and the absorbance of the supernatant was obtained at 405 nm. The solution was placed back into the reaction flask, and the process was repeated for 6 min.

For dry Fe$_3$O$_4$@silica-αCT stored at 4 °C, 1.0 mg of Fe$_3$O$_4$@silica-αCT was resuspended in 0.2 mL of phosphate buffer (pH 7.4) and incubated with 2.8 mL of substrate (0.4 g L^{-1}) under shaking at room temperature. After 3 min, the solid phase was magnetically separated; the solution was decanted, and its absorbance was obtained at 405 nm. The solution was placed back into the reaction flask and was incubated under shaking at room temperature was repeated for 6 min. The assays were performed in triplicate.

Chemical stability of αCT and Fe$_3$O$_4$@silica-αCT using Bz-DL-Tyr-pNA as substrate

The amidase activity of αCT stored in solution at room temperature, of dry Fe$_3$O$_4$@silica-αCT stored at 4 °C, and of Fe$_3$O$_4$@silica stored in suspension at room temperature or at 4 °C were measured using Bz-DL-Tyr-pNA as a substrate, as described above.

Reuse of Fe_3O_4@silica-αCT using Bz-DL-Tyr-*p*NA as substrate

After use, Fe_3O_4@silica-αCT was magnetically separated from the reaction medium; the solution was removed, and the solid was washed with phosphate buffer (50 mmol L^{-1}, pH 7.4). A fresh substrate solution was added to it to measure enzyme activity, as described above.

Transmission electron microscopy (TEM)

The sample was prepared in a carbon-coated copper grid by adding a drop of an ethanol suspension containing the material. TEM was performed using a Philips CM 200 microscope (Philips, Amsterdam, Netherlands) operating at 200 kV.

Enzyme activity assay using Suc-AAPF-*p*NA as substrate

Due to practical advantages, Suc-AAPF-*p*NA was used as a substrate in the determination of αCT thermal stability and kinetics parameters.

For the free αCT, 2 μL of fresh enzyme solution (0.05 mg mL^{-1} in Tris–HCl 100 mmol L^{-1} buffer pH 8), 8μL of Tris–HCl buffer pH 8, and 200 μL of substrate solution (0.3 mg mL^{-1} Suc-AAPF-*p*-NA in DMSO and Tris–HCl buffer pH 8) were incubated at 37 °C under shaking in an ELISA microplate. The reaction was monitored in a BioTek ELx800 Absorbance Microplate Reader (Winooski, USA) coupled to a computer to record the absorbance variation at 415 nm. The reaction was ended by the addition of 30 % HAc solution (Sigma Chemical Co., USA) in 5-min intervals for 30 min. Each reaction had a set of three blanks: one with substrate solution, another with αCT, and another with HAc; Tris–HCl buffer was added to reach final volumes of 250 μL.

For wet Fe_3O_4@silica-αCT, 2 μL of Fe_3O_4@silica-αCT suspension stored at room temperature (5 mg mL^{-1}), 8 μL of Tris–HCl buffer, and 200 μL of substrate solution (0.3 mg mL^{-1} Suc-AAPF-*p*-NA in DMSO and Tris–HCl buffer pH 8) were incubated at 37 °C under shaking in an ELISA microplate. The reaction was ended by the addition of a 30 % HAc solution (Sigma Chemical Co., USA) in 5-min intervals for 30 min. After 30 min, Fe_3O_4@silica-αCT was magnetically separated and the absorbance

of the supernatant of each well was obtained at 415 nm. A set of three blanks, as described above, was used.

The assays were performed in triplicate. Absorbances were obtained in a SpectraMax® Paradigm® multi-mode detection platform (Lagerhausstrasse, Austria). Quantification of the product (*p*NA) was done using a calibration curve obtained for *p*NA with concentrations varying from 5 to 500 μmol L^{-1}.

Determination of thermal stability of αCT and of Fe_3O_4@silica-αCT using Suc-AAPF-*p*NA as substrate

Fresh free αCT (0.5 mg mL^{-1}) and Fe_3O_4@silica-αCT (suspension stored at room temperature, 5.0 mg mL^{-1}) were previously incubated in a shaker at 60 °C for 12 h. Aliquots were removed every 10 min for the first hour of reaction and every hour for the next 11 h. Each aliquot had its amidase activity upon Suc-AAPF-*p*NA determined following the procedure described above.

Determination of enzyme kinetics parameters for αCT and Fe_3O_4@silica-αCT using Suc-AAPF-*p*NA as substrate

Suc-AAPF-*p*NA solutions with concentrations varying from 20 to 800 μmol L^{-1} were incubated with the enzyme for αCT (0.5 mg mL^{-1}) or Fe_3O_4@silica-αCT stored at room temperature (5.0 mg mL^{-1}) following the experimental conditions described above. The initial rates of hydrolysis of these substrate samples were fitted into the Michaelis–Menten equation using the Enzfitter software, resulting in the K_m and K_{cat} parameters.

Hydrolysis of the methyl ester of Z-Ala-Phe-OMe catalyzed by Fe_3O_4@silica-αCT

The Fe_3O_4@silica-αCT suspension stored at room temperature (0.2 mL) was placed in a flask; the solid was retained magnetically, and the buffer was removed. Then, 3.0 mL of 30 % ACN/NaH_2PO_4 buffer (pH 8) and Z-Ala-Phe-OMe (0.04 mol L^{-1}) were added to the reaction flask. The mixture was stirred (300 rpm) at 37 °C. Diluted aliquots were analyzed by reversed-phase high-performance liquid chromatography (RP-HPLC) and by RP-HPLC coupled to mass spectrometry with electrospray ionization (LC/ESI–MS) at 0, 15, 30, 60, and 120 min.

The RP-HPLC analyses were completed using a C18 Vydac column (0.46 cm × 25.00 cm, 5 μmol L^{-1}, 300 Å, USA) that employed a system composed of Constametric 3500 and 3200 pumps from Thermo Separation Products (TSP, USA), an automatic sampler Spectrasystem AS3000 from TSP, a Spectromonitor 3100 detector from LDC Analytical or a Tunable Absorbance Detector 486 from Waters (USA), and a Data Jet integrator from TSP (USA). The separation of compounds (reactants and products) occurred in linear gradients (5–95 % B) using 0.1 % TFA in water (solvent A) and 60 % ACN/0.09 % TFA in water (solvent B). The flow used was 1 mL min^{-1} and the wavelength (λ) was 210 nm. The LC–MS analyses used the same column but the following equipment: (1) a Shimadzu liquid chromatographer composed of two Shimadzu LC-10AD pumps and a Shimadzu SDP-10AV detector; and (2) a Micromass Quatro II triple quadrupole mass spectrometer (Altricham, UK). The software Mass-Linx™ for Windows NT® was used in the analysis of the mass spectra obtained.

Results and discussion

Choice and preparation of the magnetic support

The first step of this study was to choose a magnetic carrier for the immobilization of αCT. The appropriate choice of magnetic carriers and immobilization strategy can dramatically increase the efficiency of the separation process. The selection criteria should rely on materials' quality (morphology, size, and dispersion) and magnetic properties. SPM NPs are strongly attracted to an applied magnetic field due to the contribution of large magnetic moments within the individual particles, but removal of the applied magnetic field instantaneously reduces the overall magnetic moment back to zero. Additionally, SPM NPs may not be stable under reaction conditions employed in organic synthesis, and their coating with a layer of different materials (carbon, metal, oxides, etc.) provides an effective barrier against oxidation and acid corrosion (Rossi et al. 2014).

We chose to use well-defined and size-controlled silica-coated SPM NPs. Coating the magnetite NP surface with a layer of silica is a strategy for protecting the magnetic content, avoiding unwanted interactions and magnetite oxidation. Furthermore, silica facilitates the immobilization of enzymes through a covalent approach. The method used here for the coating of magnetite with silica and reported previously by some of us (Jacinto et al. 2008) is based in a reverse micellar microemulsion, which is very efficient, reproducible, and easy to scale up, while providing a well-defined core–shell morphology in a nanometric scale—not easily obtained using other sol–gel or polymerization methods (Rossi et al. 2014). The magnetite cores (Fe$_3$O$_4$ ∼ 10 nm, Fig. 1a) were easily synthesized by a co-precipitation method, which provided a superparamagnetic material with a saturation magnetization (Ms) of 62 emu/g (Rossi et al. 2007). This material was spherically coated with silica (spheres of ∼ 50 nm in diameter, Fig. 1b) and maintained their magnetic properties (M_s = 9 emu/g (total mass of material) at 300 K, which corresponds to 69 emu/g of Fe$_3$O$_4$ (Jacinto et al. 2009)). The material displays excellent magnetic properties, such as very low coercivity field and high saturation magnetization, allowing its recovery from the reaction media by applying a magnetic field and easily redispersion after the removal of the magnetic field. Repeated cycles of separation and dispersion are possible because of the absence of magnetic memory. An overview of our previous studies on the design and modification of superparamagnetic nanomaterials for application in the field of magnetic separation and catalysis can be found elsewhere (Rossi et al. 2012).

Functionalization of magnetic support and the covalent immobilization of its αCT

As shown in Scheme 1, the synthetic process comprised the functionalization of silica-coated magnetite NPs with amino groups (1st step) and enzyme immobilization using the cross-linking reagent glutaraldehyde (2nd and 3rd steps).

In the first step, reaction with 3-aminopropyltriethoxysilane (APTES) provided the amino groups on the silica surface, the quantification of which was carried out by the ninhydrin method (Kaiser et al. 1970; Taylor and Howard 1993) using a calibration curve obtained with a solution of a variable concentration of free APTES. The result was 55 nmol NH$_2$/100 mg$_{support}$.
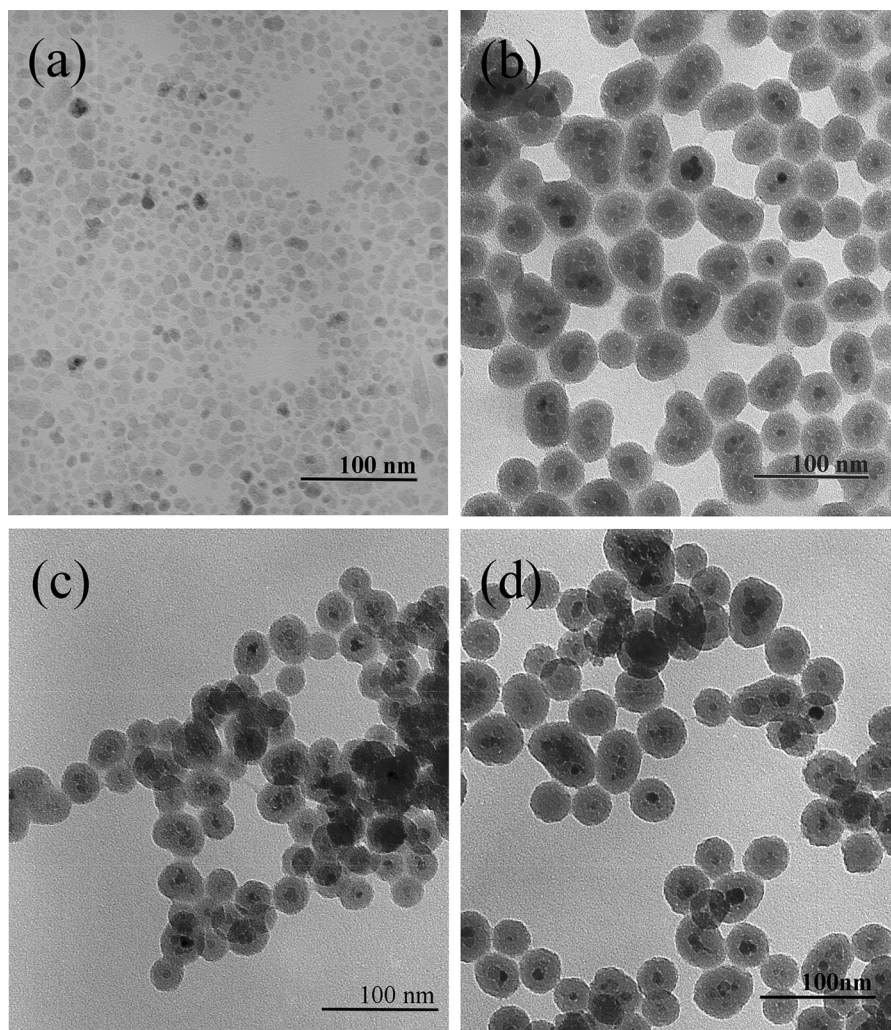
Fig. 1 TEM images of **a** oleic acid-coated Fe$_3$O$_4$, **b** Fe$_3$O$_4$@silica, **c** fresh Fe$_3$O$_4$@silica-αCT and **d** Fe$_3$O$_4$@silica-αCT after 103 days of storage

In the second step, amino groups of the support were further reacted with glutaraldehyde to provide free aldehyde groups to react with amino groups of the enzyme (3rd step), promoting a covalent linkage between it and the nanoparticle (Rossi et al. 2004). In fact, it is well known that glutaraldehyde can easily react with amino groups of lysines, amino acids present in the structure of proteins and enzymes (Migneault et al. 2004). After the reaction with glutaraldehyde, the ninhydrin method indicated 44 nmol NH$_2$/100 mg$_{support}$ or a yield of 20 % (or 1.1×10^{-5} mol$_{glutaraldehyde}$/100 mg$_{support}$).
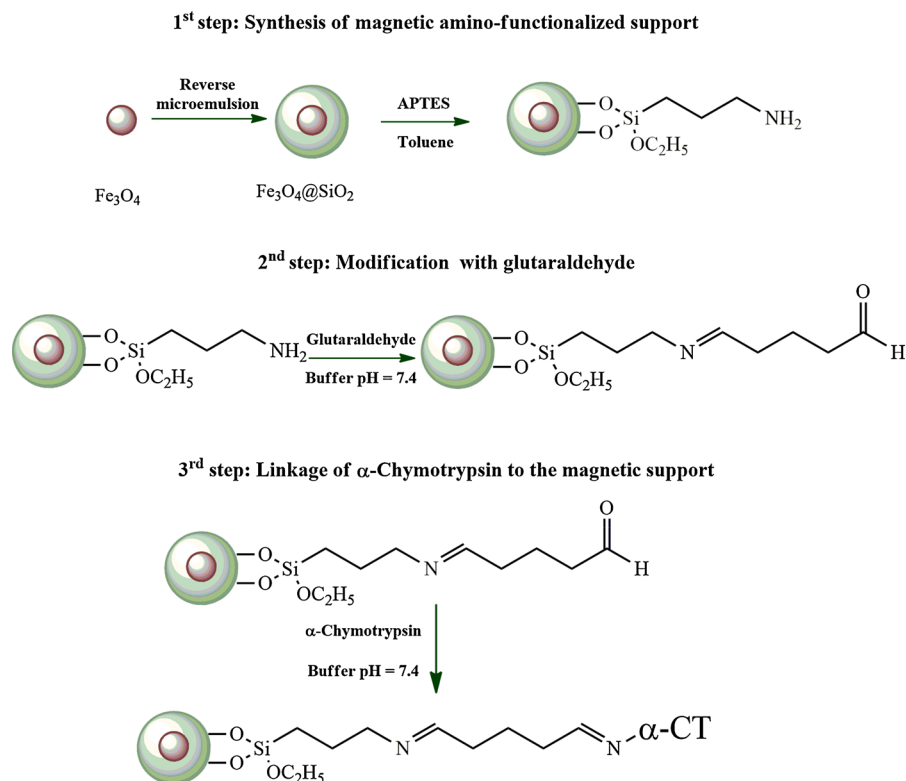
The last step, responsible for binding the protease αCT to the glutaraldehyde-activated support, resulted in a suspension of 3.4 mg solid mL^{-1} of phosphate

buffer. The supported Fe$_3$O$_4$@silica-αCT was easily recovered from the reaction media using a magnet, and it was then tested against the substrate Bz-DL-Tyr-pNA or Suc-AAPF-*p*NA. The amidase activity indicated that immobilization was successful.

Determination of protein content in the magnetic carrier: establishment of a new method for such purpose

Protein contents of immobilized enzymes can be determined by several methods, such as those of Lowry (Leão et al. 1991), Bradford (Palocci et al. 2007; Netto et al. 2009), bicinchoninic acid (BCA) (Chen and Su 2001; Hong et al. 2007a, b), and UV

Scheme 1 Preparation of αCT covalently bound to superparamagnetic nanoparticle

1st step: Synthesis of magnetic amino-functionalized support

Fe₃O₄ → Reverse microemulsion → Fe₃O₄@SiO₂ → APTES / Toluene →

2nd step: Modification with glutaraldehyde

Glutaraldehyde / Buffer pH = 7.4

3rd step: Linkage of α-Chymotrypsin to the magnetic support

α-Chymotrypsin / Buffer pH = 7.4

absorption spectroscopy (Rossi et al. 2004). The fluorogenic reagent 4-methylumbelliferyl *p*-(*N,N,N*-trimethylammonium cinnamate) (MUTMAC) can also be used for this purpose (Clark and Bailey 2002). The general procedure is to measure the free enzyme content of the immobilization solution at the beginning of the reaction and after draining/washing the solid support.

In this study, the amount of immobilized enzyme was initially measured using the Bradford method. As shown in Table 1, the results suggested an immobilization yield close to 90 %. Such high yield was not expected and encouraged further studies with the enzyme-nanoparticle hybrid material because αCT is an autolytic enzyme. In fact, the theoretical proteolysis of free αCT originated up to 19 peptide fragments, with MW <3,400 that likely do not react with the Bradford reagent as efficiently as the intact enzyme does.

The total acid hydrolysis followed by amino acid analysis of the hydrolyzate showed to be a more robust and consistent method as the results obtained for the magnetic support before enzyme immobilization (negative control), for the free αCT at 0 h of immobilization, and for the αCT-nanoparticle hybrid

Table 1 Quantification of free αCT present in the immobilization reaction medium at 0 and 2 h using standard Bradford protein assay

0 h (mg enzyme/ mg support)	2 h (mg enzyme/ mg support)	Difference (mg/mg support)
0.133 ± 0.027	0.013 ± 0.006	0.120

These results were obtained using a calibration curve established with bovine serum albumin ($y = 0.039x - 0.015$)

material obtained after 2 h of immobilization were quite reproducible (Table 2). Therefore, we propose this method as a reliable alternative for quantifying the amount of protein bound to magnetite NPs.

Comparative chemical stability of free αCT and Fe₃O₄@silica-αCT

Chemical stability is a key property to be examined in enzyme immobilization studies, as an increased chemical stability favors storage and reuse of the immobilized enzyme (Kim et al. 2005; Rossi et al. 2004; Netto et al. 2009; Hong et al. 2007a, b; Lee et al. 2009). Figure 2 shows the results of amidase activity

Table 2 Kinetics of αCT immobilization on Fe$_3$O$_4$@silica

Reaction time (h)	Immobilized αCT[a] (nmol enzyme/mg nanoparticle)	Immobilization yield (%)
0	0.0	0
2	1.6	21
4	1.5	20
8	1.7	22
16	1.7	22

[a] The amount of αCT added per mg of Fe$_3$O$_4$@silica was 7.6 nmol. Enzyme contents were obtained by the full hydrolysis of Fe$_3$O$_4$@silica-αCT followed by HPLC amino acid analysis of the hydrolyzate

using Bz-DL-Tyr-pNA as substrate along the storage time. Despite being significantly more active (2.6 times) than the immobilized enzyme, fresh free αCT was less stable in solution due to autolysis (activity reduction in 24 h: 90 %). Conversely, Fe$_3$O$_4$@silica-αCT activity did not change considerably in 90 days independently whether stored in dry form or in suspension at room temperature or at 4 °C, revealing a drastic diminution of αCT autolysis. When stored in suspension at room temperature, Fe$_3$O$_4$@silica-αCT presented a smaller reduction (20 % in 178 days) of its initial amidase activity, which is probably related to protein denaturation. However, when kept dry, the immobilized enzyme had its amidase activity significantly decreased (about 60 % of its initial value), a result that is probably associated with protein dehydration and irreversible denaturation. In summary, even less active than free αCT, Fe$_3$O$_4$@silica-αCT remains as such for about 6 months when stored in suspension at room temperature; so this is the best condition for its storage.

These results are in agreement with previous reports of immobilized αCT activity maintenance for 6–36 days of storage under shaking at room temperature (Kim et al. 2005; Lee et al. 2009; Hong et al. 2008). However, the supports and immobilization procedures used by the authors of those studies are different or only slightly similar (Kim et al. 2005) to those employed in this study.

Fe$_3$O$_4$@silica-αCT reuse

Figure 3 shows that Fe$_3$O$_4$@silica-αCT stored in suspension at room temperature displayed no significant modification in enzymatic activity after 10 cycles
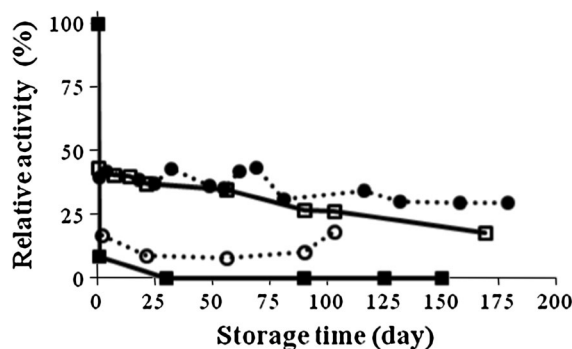

Fig. 2 Stabilities of fresh free αCT and Fe$_3$O$_4$@silica-αCT stored at different conditions. The figure shows αCT stored at room temperature (*filled square*; Fe$_3$O$_4$@silica-αCT stored in suspension at room temperature (*open square*); Fe$_3$O$_4$@silica-αCT stored in suspension at 4 °C (*filled circle*); and Fe$_3$O$_4$@-silica-αCT stored dry at 4 °C (*open circle*). The relative activity (%) represents the ratio of residual activity/initial activity of αCT

of reutilization, indicating an advantage of this type of immobilization. These results are very promising since previous studies on the immobilization of αCT in other types of nanoparticles and other attempts to reuse the protease-NPs for successive cycles show significant activity loss (around 30 % of the initial activity) as a function of the number of cycles (Ju et al. 2012). Moreover, these results are in agreement with observations made by other authors about preservation of αCT amidase activity after immobilization on solid supports different from ours in 5 cycles of use (Li et al. 2013; Hong et al. 2007a, b) and 30 cycles of use (Kim et al. 2005; Lee et al. 2009; El-Ghaffar and Hashem 2013).

Morphology of Fe$_3$O$_4$@silica-αCT

Magnetic recovery of the immobilized enzyme from the reaction media was easy and quantitative, suggesting the maintenance of material integrity and magnetic properties. To identify possible morphological changes of the nanoparticles after the storage of Fe$_3$O$_4$@silica-αCT, Transmission Electron Microscopy (TEM) images were obtained for the fresh and after 103 days of storage (Fig. 1c, d). No morphological changes of the nanoparticles were detected, when compared to the Fe$_3$O$_4$@silica (Fig. 1b), revealing that either αCT immobilization or storage did not
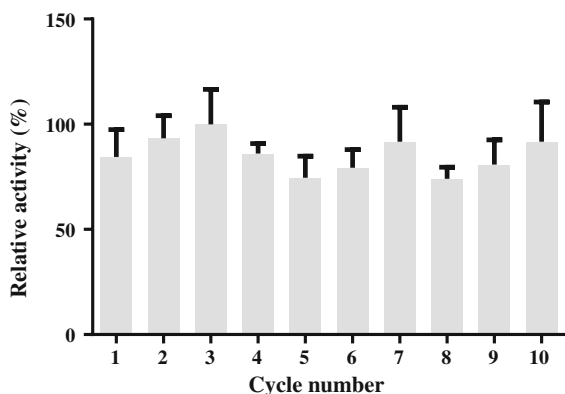
Fig. 3 Relative amidase activity measured after use of Fe₃O₄@silica-αCT stored in suspension at room temperature for ten cycles. The analysis of variance (ANOVA) gave a very high *p* value ($p = 0.2481$)

caused any apparent physical damage to the *core–shell* nanostructure.

Comparative thermal stability of free αCT and Fe₃O₄@silica-αCT using Suc-AAPF-*p*NA as substrate

Suspecting that enzyme immobilization would affect proteins' irreversible denaturation, autolysis, or both, Fe₃O₄@silica-αCT was stored in suspension at room temperature; fresh free αCT had their amidase activity measured after pre-incubation at 60 °C for 12 h. Figure 4 reveals that the immobilized enzyme displayed higher thermal stability since, after 1 h under heating, the free enzyme was completely inactivated, while the magnetically separable enzyme retained ca. 30 % of its initial activity.

These results not only confirm that immobilization reduces protein denaturation and/or autolysis rates but also suggest that structural protection resulting from covalent binding between αCT and NPs (which involve the amino group of lysine side chain) hinders enzyme–enzyme interactions. Indeed, immobilization on solid support limits enzyme diffusion in solution and makes it less accessible to larger substrates due to structural steric hindrance (Arica et al. 2004).
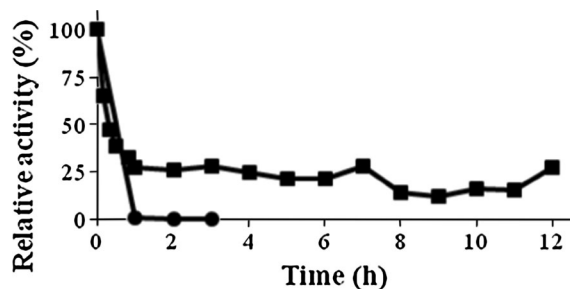

Fig. 4 Thermal stability of free αCT (*filled circle*) and Fe₃O₄@silica-αCT (*filled square*). Remaining amidase activity was determined after enzyme pre-incubation at 60 °C. The remaining activity (%) represents the ratio of residual activity after pre-incubation/initial activity

Moreover, the results described above corroborate previous observations of enhancement of αCT stability when this protease was immobilized in nanometer-scale composites and magnetite nanoparticles different from ours (Kim et al. 2005). Additionally, Yao and coworkers (Hong et al. 2006) along with other authors (Arica et al. 2004; Mateo et al. 2000) observed increment on αCT thermal stability due to immobilization, which further supports our data.

Determination of kinetics parameters for αCT and Fe₃O₄@silica-αCT as catalyst of amide bond hydrolysis

The effect of substrate concentration on the amidase activity of fresh free αCT and its immobilized form were also evaluated in the present study, providing the kinetic constants K_{cat} (catalytic rate constant), K_m (Michaelis–Menten constant), and $K_{cat} \cdot K_m^{-1}$ (Table 3). No significant change was observed in the K_m, whereas the K_{cat} for the immobilized αCT dropped (25-fold). These data suggest the following: (i) only part of the immobilized αCT binds the substrate and catalyzes the hydrolysis because the immobilization on the NPs through lysine residues did not affect all enzyme molecules equally (according to the protein data bank (PDB), bovine αCT has 14 lysine residues

Table 3 Kinetics parameters for free αCT and for Fe₃O₄@silica-αCT	K_m (mol L⁻¹)	K_{cat} (min⁻¹)	$K_{cat} \cdot K_m^{-1}$ (min⁻¹ L mol⁻¹)
Free αCT	$4.0 \times 10^{-4} \pm (0.5)$	$2.21 \times 10^{3} \pm (0.09)$	$5.5 \times 10^{6} \pm (0.9)$
Fe₃O₄@silica-αCT	$5.3 \times 10^{-4} \pm (0.7)$	$0.089 \times 10^{3} \pm (0.005)$	$0.17 \times 10^{6} \pm (0.03)$

that could be involved in the reaction with glutaral-dehyde-activated NPs (Tsukada and Blow 1985)); and (ii) the binding to the NPs caused changes in the enzyme structure that did not affect enzyme affinity for the substrate, but somehow modified its efficiency to catalyze amide bond hydrolysis.

Modification of the kinetic constants K_m and K_{cat} for proteases due to their immobilization has also been previously described and was associated with enzyme structural changes and the diminution of enzyme diffusion (Hong et al. 2007a, b).

Fe$_3$O$_4$@silica-αCT as a reusable catalyst in peptide ester hydrolysis

Because bioactive peptides and analogs have been routinely synthesized in our laboratory using the chemical methods (peptide synthesis in solution and solid-phase peptide synthesis (Chandrudu et al. 2013)), we know that, despite their categorical efficiency, these technologies are not as environmentally friendly as desired. We therefore performed a few steps of the synthetic process with the help of enzymes, a cleaner

technology. Indeed, proteases with esterase activity such as αCT have been successfully used to catalyze the formation and hydrolysis of amide bonds and ester bonds, reactions mostly required in enzymatic peptide synthesis (Miranda and Tominaga 1991; Liria et al. 2008; Narai-Kanayama et al. 2012). Yet enzymes have short lifetimes, high costs, and are difficult to recycle, hampering the general use of this clean technology.

Knowing that αCT is a well-known enzyme that specifically catalyzes hydrolysis of peptide bonds and peptide esters involving the carboxyl group of aromatic amino acids and having observed in the present study that Fe$_3$O$_4$@silica-αCT exhibited significant amidase activity and reduced autolysis as well as reasonable enhancement of protein thermal stability, we became interested in verifying whether it, so easily recoverable from reaction media by magnetism, had the potential to act as a powerful catalyst of ester hydrolysis, one of the steps of enzymatic peptide synthesis. Thus, the protected dipeptide Z-Ala-Phe-OMe (1) was incubated with Fe$_3$O$_4$@silica-αCT stored in suspension at room temperature. As can be seen in Fig. 5, peak 1 decreased and peak 2 appeared/
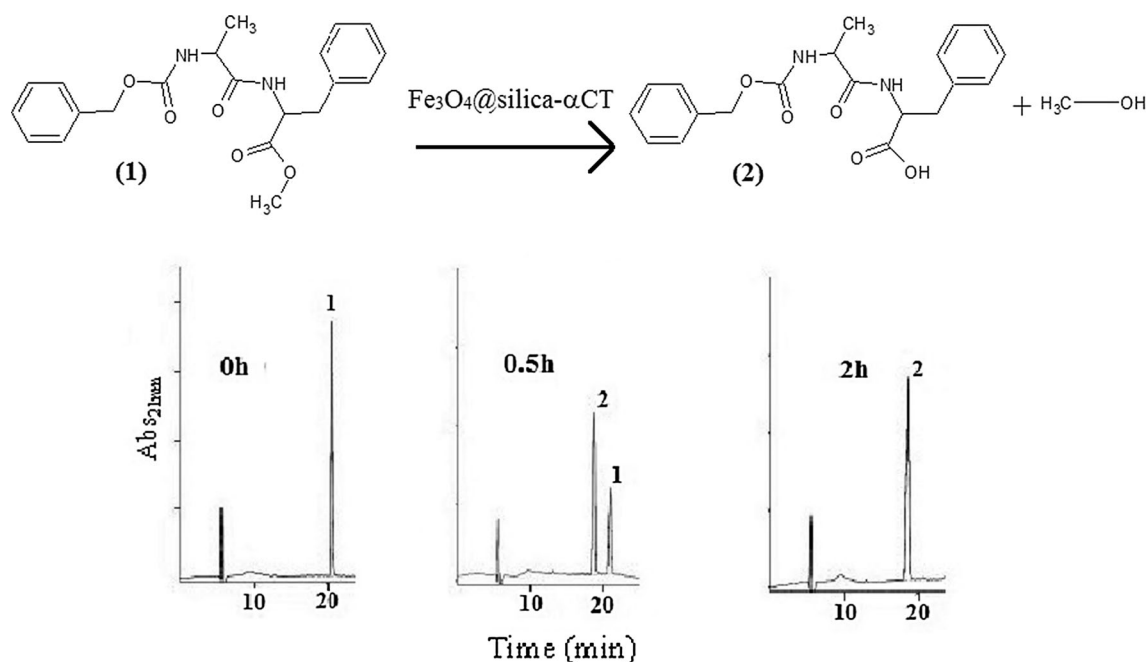
Fig. 5 Monitoring of Z-Ala-Phe-OMe ester hydrolysis catalyzed by Fe$_3$O$_4$@silica-αCT. RP-HPLC conditions are as follows: column Vydac C$_{18}$, solvent A: 0.1 % TFA/H$_2$O, B: 80 % ACN/0.09 % TFA/H$_2$O, flow: 1 mL min^{-1}, gradient: 5–95 % of B in 30 min, λ: 210 nm. ESI–MS conditions are as follows: capillary voltage: 2 kV, cone voltage: 15 kV, ionization mode: ES+. *Section* (**1**) shows Z-Ala-Phe-OMe, *m/z* [M+H$^+$] (calculated/obtained): 384.9/385.2; *section* (**2**) shows Z-Ala-Phe, *m/z* [M+H$^+$] (calculated/obtained): 370.0/371.2

increased with reaction time, suggesting efficient ester hydrolysis. This was confirmed using an LC/ESI–MS analysis of a sample collected after 30 min of reaction. Compounds 1 and 2 are identified as Z-Ala-Phe-OMe and Z-Ala-Phe, respectively.

The immobilized enzyme was quantitatively removed from the reaction medium and was reused for the same purpose for at least four cycles.

Conclusion

The novelties of the present study are the following: (i) we used methods, procedures, and the superparamagnetic nanoparticles Fe_3O_4@silica previously described to demonstrate that a protease/esterase, such as bovine αCT, can be easily immobilized to offer another active, suitably stable, easy to recover from the reaction media, and reusable biocatalyst; (ii) we showed that full acid hydrolysis followed by amino acid analysis of the hydrolyzate is a consistent method to quantify the protein content of magnetite NPs-proteases; and (iii) we demonstrated that the improvements achieved by immobilized αCT are promising for the development of greener chemical procedures. The observed suitability Fe_3O_4@silica-αCT as catalyst of amide bond hydrolysis or ester bond hydrolysis using amino acids or peptide derivatives as reagents evidences its practical potential in peptide synthesis, protein chemistry, proteomics, and organic synthesis.

References

Aldridge S (2013) Industry backs biocatalysis for greener manufacturing. Nat Biotechnol 31(2):95–96

Arica MY, Bayramoglu G, Biçak N (2004) Characterisation of tyrosinase immobilised onto spacer-arm attached glycidyl methacrylate-based reactive microbeads. Process Biochem 39:2007–2017

Bernal C, Illanes A, Wilson L (2014) Heterofunctional hydrophilic–hydrophobic porous silica as support for multipoint covalent immobilization of lipases: application to lactulose palmitate synthesis. Langmuir 30:3557–3566

Bundy HF (1863) Chymotrypsin-catalyzed hydrolysis of N-acetyl- and N-benzoyl-L-tyrosine p-nitroanilides. Arch Biochem Biophys 102:416–422

Chandrudu S, Simerska P, Toth I (2013) Chemical methods for peptide and protein production. Molecules 18:4373–4388

Chen JP, Su DR (2001) Latex particles with thermo-flocculation and magnetic properties for immobilization of alpha-chymotrypsin. Biotechnol Prog 17:369–375

Christian MS, Brent RL (2001) Teratogen update: evaluation of the reproductive and developmental risks of caffeine. Teratology 64(1):51–78

Clark DS, Bailey JE (2002) Structure-function relationships in immobilized chymotrypsin catalysis. Biotechnol Bioeng 79:539–549

Datta S, Christena LR, Rajaram YSR (2013) Enzyme immobilization: an overview on techniques and support materials. 3 Biotech 3:1–9

El-Ghaffar MAA, Hashem MS (2013) Calcium alginate beads encapsulated PMMA-g-CS nano-particles for α-chymotrypsin immobilization. Carbohydr Polym 92:2095–2102

Faber K (1997) Biotransformations in organic chemistry. Springer, Berlin

Flores-Fernández GM, Griebenow K (2012) Glycosylation improves α-chymotrypsin stability upon encapsulation in poly(lactic-co-glycolic)acid microspheres results. Pharma Sci 2:46–51

Forsberg EM, Green JRA, Brennan JD (2011) Continuous flow immobilized enzyme reactor-tandem mass spectrometry for screening of AChE inhibitors in complex mixtures. Anal Chem 83:5230–5236

Hegedus I, Nagy E (2009) Improvement of chymotrypsin enzyme stability as single enzyme nanoparticles. Chem Eng Sci 64:1053–1060

Homaei AA, Sariri R, Vianello F, Stevanato R (2013) Enzyme immobilization: an update. J Chem Biol 6:185–205

Hong J, Gong PJ, Yu JH, Xua DM, Suna HW, Yao S (2006) Conjugation of α-chymotrypsin on a polymeric hydrophilic nanolayer covering magnetic nanoparticles. J Mol Catal B 42:99–105

Hong J, Gonga P, Xu D, Donga L, Yao S (2007a) Stabilization of α-chymotrypsin by covalent immobilization on amine-functionalized superparamagnetic nanogel. J Biotechnol 128:597–605

Hong J, Xu D, Gong P, Sun H, Dong L, Yao S (2007b) Covalent binding of α-chymotrypsin on the magnetic nanogels covered by amino groups. J Mol Catal B 45:84–90

Hong J, Xu D, Gong P, Yu J, Ma H, Yao S (2008) Covalent-bonded immobilization of enzyme on hydrophilic polymer covering magnetic nanogels. Microporous Mesoporous Mater 109:470–477

Jacinto MJ, Kiyohara PK, Masunaga SH, Jardim RF, Rossi LM (2008) Recoverable rhodium nanoparticles: synthesis, characterization and catalytic performance in hydrogenation reactions. Appl Catal A 338:52–57

Jacinto MJ, Santos OHCF, Jardim RF, Landers R, Rossi LM (2009) Preparation of recoverable Ru catalysts for liquid-phase oxidation and hydrogenation reactions. Appl Catal A 360:177–182

Ju HY, Kuo CH, Too JR, Huanh HY, Twu YK, Chang CMJ, Liu YC, Shieh CJ (2012) Optimal covalent immobilization of α-chymotrypsin on Fe_3O_4-chitosan nanoparticles. J Mol Catal B 78:9–15

Kaiser E, Colescott RL, Bossinger CD, Cook PI (1970) Color test for detection of free terminal amino groups in the solid-phase synthesis of peptides. Anal Biochem 34(2):595–598

Kim J, Lee J, Na HB, Kim BC, Youn JK, Kwak JH, Moon K, Lee E, Kim J, Park J, Dohnalkova A, Park HG, Gu MB, Chang H, Grate JW, Hyeon TA (2005) A magnetically separable, highly stable enzyme system based on nanocomposites of enzymes and magnetic nanoparticles shipped in hierarchically ordered, mesocellular, mesoporous silica. Small 12:1203–1207

Leão AMAC, Oliveira EA, Carvalho LB Jr (1991) Immobilization of protein on ferromagnetic dacron. Appl Biochem Biotechnol 31:53–58

Lee J, Na HB, Kim BC, Lee JH, Lee B, Kwak JH, Hwang Y, Park J-G, Gu MB, Kim J, Joo J, Shin C-H, Grate JW, Hyeon T, Kim J (2009) Magnetically-separable and highly-stable enzyme system based on crosslinked enzyme aggregates shipped in magnetite-coated mesoporous silica. J Mater Chem 19:7864–7870

Li DF, Ding HC, Zhou T (2013) Covalent immobilization of mixed proteases, trypsin and chymotrypsin, onto modified polyvinyl chloride microspheres. J Agric Food Chem 61:10447–10453

Liria CW, Romagna CD, Rodovalho NN, Marana SR, Miranda MTM (2008) Dipeptide synthesis in biphasic medium: evaluating the use of commercial porcine pancreatic lipase preparations and the involvement of contaminant proteases. J Braz Chem Soc 19:1574–1581

Lugo-Morales LZ, Loziuk PL, Corder AK, Toups JV, Roberts JG, McCaffrey KA, Sombers LA (2013) Enzyme-modified carbon-fiber microelectrode for the quantification of dynamic fluctuations of nonelectroactive analytes using fast-scan cyclic voltammetry. Anal Chem 85:8780–8786

Machini MT (1985) Termolisina como catalisador na síntese de di-e tripeptídeos contendo asparagina. MSc Thesis, University of São Paulo, São Paulo

Mateo C, Abian O, Fernandez-Lafuente R, Guisan JM (2000) Increase in conformational stability of enzymes immobilized on epoxy-activated supports by favoring additional multipoint covalent attachment. Enzyme Microb Technol 26:509–515

Migneault I, Dartiguenave C, Bertrand MJ, Waldron KC (2004) Glutaraldehyde: behavior in aqueous solution, reaction with proteins, and application to enzyme crosslinking. Biotechniques 37(4):790–802

Miranda MTM, Tominaga M (1991) Thermolysin as a catalyst in enzymatic synthesis of asparagine-containing peptides II. Int J Pept Protein Res 37(2):128–133

Miranda MTM, Cheng E, Muradian J, Seidel WF, Tominaga M (1986) Thermolysin as a catalyst in enzymatic synthesis of asparagine-containing peptides. Bioorg Chem 14(2):182–193

Narai-Kanayama A, Hanaishi T, Aso K (2012) α-Chymotrypsin-catalyzed synthesis of poly-L-cysteine in a frozen aqueous solution. J Biotechnol 157:428–436

Netto CGCM, Andrade LH, Toma HE (2009) Enantioselective transesterification catalysis by Candida antarctica lipase immobilized on superparamagnetic nanoparticles. Tetrahedron Asymmetry 20:2299–2304

Netto CGCM, Toma HE, Andrade LH (2013) Superparamagnetic nanoparticles as versatile carriers and supporting materials for enzymes. J Mol Catal B 85–86:71–92

Palocci C, Chronopoulou L, Venditti I, Cernia E, Diociaiuti M, Fratoddi I, Russo MV (2007) Lipolytic enzymes with improved activity and selectivity upon adsorption on polymeric nanoparticles. Biomacromolecules 8:3047–3053

Pankhurst QA, Connolly J, Jones SK, Dobson J (2003) Applications of magnetic nanoparticles in biomedicine. J Phys D Appl Phys 36:167–181

Rossi LM, Quach AD, Rosenzweig Z (2004) Glucose oxidase–magnetite nanoparticle bioconjugate for glucose sensing. Anal Bioanal Chem 380:606–613

Rossi LM, Vono LLR, Silva FP, Kiyohara PK, Duarte EL, Matos JR (2007) A magnetically recoverable scavenger for palladium based on thiol-modified magnetite nanoparticles. Appl Catal A 330:139–144

Rossi LM, Garcia MAS, Vono LLR (2012) Recent advances in the development of magnetically recoverable metal nanoparticle catalysts. J Braz Chem Soc 23:1959–1971

Rossi LM, Costa NJS, Silva FP, Wojcieszak R (2014) Magnetic nanomaterials in catalysis: advanced catalysts for magnetic separation and beyond. Green Chem 16:2906–2933

Singh RK, Tiwari MK, Singh R, Lee JK (2013) From protein engineering to immobilization: promising strategies for the upgrade of industrial enzymes. Int J Mol Sci 14:1232–1277

Sun J, Hu K, Liu Y, Pan Y, Yang Y (2013) Novel superparamagnetic sanoparticles for trypsin immobilization and the application for efficient proteolysis. J Chromatogr B 942–943:9–14

Taylor I, Howard AG (1993) Measurement of primary amine groups on surface-modified silica and their role in metal binding. Anal Chim Acta 271:77–82

Thomas SM, DiCosmo R, Nagarajan V (2002) Biocatalysis: applications and potentials for the chemical industry. Trends Biotechnol 20(6):238–242

Tsukada H, Blow DM (1985) Structure of α-chymotrypsin refined at 1.68 Å resolution. J Mol Biol 184:703–711

Yamaguchi H, Miyazaki M, Kawazumi H, Maeda H (2010) Multidigestion in continuous flow tandem protease-immobilized microreactors for proteomic analysis. Anal Biochem 407:12–18

Zhang A, Ye F, Lu J, Zhao S (2013) Screening α-glucosidase inhibitor from natural products by capillary electrophoresis with immobilised enzyme onto polymer monolith modified by gold nanoparticles. Food Chem 141:1854–1859